 CMES, vol.84, no.5, pp.459-497, 2012

A Simple Collocation Scheme for Obtaining the Periodic Solutions of the Duffing Equation, and its Equivalence to the High Dimensional Harmonic Balance Method: Subharmonic Oscillations

Hong-Hua Dai[1, 2], **Matt Schnoor**[2] **and Satya N. Atluri**[2]

Abstract: In this study, the harmonic and $1/3$ subharmonic oscillations of a single degree of freedom Duffing oscillator with large nonlinearity and large damping are investigated by using a simple point collocation method applied in the time domain over a period of the periodic solution. The relationship between the proposed collocation method and the high dimensional harmonic balance method (HDHB), proposed earlier by Thomas, Dowell, and Hall (2002), is explored. *We demonstrate that the HDHB is not a kind of "harmonic balance method" but essentially a cumbersome version of the collocation method.* In using the collocation method, the collocation-resulting nonlinear algebraic equations (NAEs) are solved by the Newton-Raphson method. To start the Newton iterative process, initial values for the N harmonics approximation are provided by solving the corresponding low order harmonic approximation with the aid of Mathematica. We also introduce a generating frequency (ω_g), where by the response curves are effectively obtained. Amplitude-frequency response curves for various values of damping, nonlinearity, and force amplitude are obtained and compared to show the effect of each parameter. In addition, the time Galerkin method [the Harmonic-Balance method] is applied and compared with the presently proposed collocation method. Numerical examples confirm the simplicity and effectiveness of the present collocation scheme in the time domain.

Keywords: harmonic oscillation, $1/3$ subharmonic oscillation, Duffing equation, high dimensional harmonic balance method (HDHB), point collocation method, time Galerkin [Harmonic-Balance] method, generating frequency.

[1] College of Astronautics, Northwestern Polytechnical University, Xi'an 710072, PR China. Correspond to Email: honghuad@uci.edu.

[2] Center for Aerospace Research & Education, Department of Mechanical & Aerospace Engineering, University of California, Irvine.

1 Introduction

As discussed in the textbook by Atluri (2005), a variety of spatial discretization methods can be used to reduce linear/nonlinear partial or differential equations in spatial coordinates only (not involving time) to linear/nonlinear algebraic equations (L/NAEs). The earliest such methods are the finite-difference methods. More recent methods are based on the general concept of setting the weighted residual error in the differential equations in the spatial domain to zero. Such methods include, for example:

1. The Galerkin method [where the trial and test functions are global, of the required degree of continuity, and may be the same, or different (Petrov-Galerkin method)].

2. The collocation method [wherein the trial functions may be global or local, and are complete and continuous to the required degree, and the test functions are Dirac Delta functions in space].

3. The finite volume method [wherein the trial functions may be global or local, and are complete and continuous to the required degree, and the test functions are local Heaviside step functions].

4. The primal Galerkin finite element method [wherein the trial and test functions are both the same, both local and are complete and continuous to the required degree].

5. The hybrid/mixed finite element methods where the higher order differential equations are reduced to a set of first-order differential equations, each of which is solved by a finite-element local approximation, using similar trial and test functions.

6. The boundary-element method, which for linear problems, may reduce the dimension of discretization by one [thus, for 3-D problem, the test functions are fundamental solutions of the differential equation in an infinite domain; and the trial functions are local approximations only over the surface of the domain].

7. A variety of Meshless Local Petrov Galerkin (MLGP) methods discovered by Atluri and co-workers since 1998 [wherein the trial functions are meshless, such as partition of unity, moving least-squares, radial basis functions, etc and the test functions may be Dirac Delta functions, Heaviside functions, radial basis functions, partition of unity, etc.]. [See Atluri and Zhu (1998); Atluri and Shen (2002); Atluri (2004)].

If the partial/ordinary differential equations in both space and time coordinates are spatially discretized by any of the methods mentioned above, one obtains [See Atluri (2005)] semi-discrete linear/nonlinear coupled ordinary differential equa-

tions in time. Or, as in coupled nonlinear Duffing Oscillators, one may directly encounter coupled nonlinear ordinary differential equations (ODEs) in the time variables. These ODEs in time have to be solved for very long times, given some initial conditions at $t = 0$. Also, often times, these ODEs exhibit periodic solutions, and hence it may be sufficient to obtain the solution only in a time interval which corresponds to the period of the periodic solution. In solving the coupled system of linear/nonlinear ODEs, for obtaining the solutions for long times, one may use many many types of time-discretization methods which are totally analogous to the spatial-discretization methods mentioned above. These include:

1. The finite-difference time marching methods which may be explicit or implicit.

2. The time-Galerkin method [wherein the trial and test functions are identical, and may be approximated by time-harmonic functions, radial basis functions in time, partitions of unity in time, etc.]. When time-harmonic functions are used for both the trial and test functions, because of the orthogonality of the harmonic functions, the time Galerkin method which is applied over a period of oscillation has been popularized as the Harmonic Balance Method (HB).

3. The collocation method wherein the error in the time-differential equation is set to zero at a finite number of points. If the response of the system is assumed to be periodic, collocation may be performed at a finite number of time-points within the period of oscillation [the trial functions may be harmonic functions, radial basis, or partitions of unity]. When the number of collocation points within a period is increased, the method trends to the method of discrete or integrated least-squared error in the ODE in time.

4. The finite volume method, wherein the trial functions may be as in the collocation method. When the solution is periodic, the finite volume method may be applied only over a period of oscillation, by setting the average error in the ODEs, for the assumed trial functions, to be zero over each of several intervals of time in the period.

5. The primal finite element method in time.

6. The mixed finite element method wherein the second-order ODE in time is reduced to a system of two first-order ODEs in time, and solved by finite elements, collocation, finite volume, etc.

7. The boundary element method in time.

8. The MLPG meshless methods in time which are entirely analogous to the MLPG spatial methods mentioned earlier.

Thus, it is clear that a variety of methods may be used to solve a system of linear/nonlinear coupled ODEs in time.

In this paper we study the subharmonic oscillations in a Duffing equation [when the period of the forcing function is nearly three-times the natural frequency of the linear system] using the time-collocation method over a period, assuming harmonic as well as subharmonic Fourier series as the trial functions.

We show that the present simple notion of collocation of the error in the nonlinear ODE, with the assumed trial functions, is entirely equivalent to the so-called High Dimensional Harmonic Balance Method (HDHB) or the Time Domain Harmonic Balance Method, introduced earlier by Hall, Thomas, and Clark (2002); Thomas, Dowell, and Hall (2002).

Closed form solutions to the Duffing equation

$$\ddot{x} + \xi\dot{x} + \alpha x + \beta x^3 = F\cos\omega t, \tag{1}$$

(where ξ is the coefficient of damping, $\sqrt{\alpha}$ is the natural frequency of the linear system, ω is the frequency of the external force, β is the coefficient of the cubic nonlinearity, F is the magnitude of the external force, x is the amplitude of motion, t is the time, and $(\dot{})$ denotes a time-differentiation), are largely unknown in all but a few simple cases due to its nonlinear character. This relatively innocent looking differential equation, however, possesses a great variety of periodic solutions. The solution of Duffing's equation (1) has both periodic and transient solutions. However, most of the research is devoted to the periodic solutions. In practice, experimentalists often observe the motions to be periodic after the transients die out. In this study, we focus our attention on the periodic solutions.

Levenson (1949) first pointed out that the Duffing equation with $\xi = 0$ may possess periodic solutions with frequency equal to $1/n$ of the frequency of the impressed force for any integer n. Moriguchi and Nakamura (1983) verified this argument by numerical trials and found that for a sufficiently small ξ, subharmonic resonances of any fractional order exist. They vanish as ξ increases or β approaches zero. In this paper, other than the harmonic oscillation, the $1/3$ subharmonic oscillation, whose fundamental frequency is one-third that of the applied force, when ω in Eq. (1) is in the vicinity of 3 times $\sqrt{\alpha}$, is investigated because the nonlinear characteristic of Eq. (1) is cubic.

Since the exact analytic solution is rarely available for the nonlinear problems, many efforts have been made towards the development of the approximate analytical methods. The perturbation method was first developed by Poincare, and later the uniformly valid version, the Lindstedt-Poincare method, the averaging method, the Krylov-Bogoliubov-Mitropolsky (KBM) method and the multiple scale method [Sturrock (1957)] were constructed. These methods, however, require the existence of a small parameter in the equation, which is not available for many cases. In this paper, we consider a strong nonlinearity when β in Eq. (1) is larger than α.

Another type of approximate method is the Galerkin method in the time-domain, applied within an appropriate period of the periodic solution (otherwise known as the harmonic balance method). It presumes a Fourier series expansion for the desired periodic solution and then obtains the nonlinear algebraic equations of the coefficients by balancing each harmonic. The two harmonic approximation (i.e., a two-term approximation in the Fourier series in time) was used to investigate the property of the Duffing equation in Stoker (1950) and Hayashi (1953a,b,c). This method was also applied to analyze a harmonically excited beam by Tseng and Dugundji (1970, 1971). However, this method is practically confined to a low number of harmonics, due to the need for a large number of symbolic operations.

Urabe (1965) and Urabe and Reiter (1966) extended the harmonic balance method to find a higher fidelity approximation for the periodic solutions. Urabe (1969) also analyzed the $1/3$ subharmonic oscillation of a weakly damped Duffing equation. Unfortunately, large numbers of symbolic operations are inevitable due to the nonlinear term in the equation.

To conquer this limitation, Thomas, Dowell, and Hall (2002); Hall, Thomas, and Clark (2002) developed a high dimensional harmonic balance method (HDHB), which has been successfully applied in aeroelastic problem, time delay problem, Duffing oscillator, Van der Pol's oscillator, etc. Studies include: Thomas, Hall, and Dowell (2003); Thomas, Dowell, and Hall (2004); Liu, Dowell, Thomas, Attar, and Hall (2006); Liu, Dowell, and Hall (2007); Ekici, Hall, and Dowell (2008); Liu and Kalmár-Nagy (2010); Ekici and Hall (2011), etc. They regarded it as a variation of the harmonic balance method, that can avoid many symbolic operations. *In this paper we show that the HDHB is not a kind of "harmonic balance method"; is essentially a version of the simple collocation method presented in this paper. The collocation method is equivalent to, but simpler than, the HDHB.* In addition, the HDHB produced additional meaningless solutions [Liu, Dowell, Thomas, Attar, and Hall (2006)], which made the HDHB method sometimes not practically useful. In using the collocation method, we provide appropriate initial values by a simple approach such that only physically meaningful solutions are calculated.

In this study, we present a very simple point collocation method based on a Fourier series type trial function to find the harmonic and $1/3$ subharmonic solution of the Duffing equation with large nonlinearity. This method is simpler than those of Urabe (1969, 1965) and Urabe and Reiter (1966), since the symbolic operations are completely avoided through the use of collocation in the time domain, within a period of the oscillation. In addition, we provide deterministic initial values for a higher order harmonic approximation from its corresponding lower order harmonic solution with the aid of Mathematica. This renders the present method applicable to a strongly damped system as well. For a considered problem, the amplitude

frequency response curves are obtained by sweeping ω from a selected generating frequency ω_g back and forth. Upon using the proposed scheme, we thoroughly investigate the effects of the damping, the nonlinearity and the force amplitude, in the Duffing equation, Eq. (1).

In Section 2, we nondimensionalize a general Duffing equation to a simpler form. In Section 3, the simple point collocation method is presented and applied to find periodic solutions of harmonic and $1/3$ subharmonic oscillations. The nonlinear algebraic equations are obtained through the use of collocation in the time domain, within a period of oscillation. In Section 4, we explore the relationship between the collocation method and the HDHB, and demonstrate that the HDHB approach is actually a transformed collocation method. Section 5 provides initial values to the NAEs solver. An undamped system is analyzed by the proposed scheme in Section 6. In Section 7, the amplitude-frequency response relations for a damped Duffing equation with various values of damping, nonlinearity and force amplitude are explored. In Section 8, the time Galerkin method [Harmonic Balance Method] is presented and applied to compare with the collocation method developed in the present paper. Finally, we come to some conclusions in Section 9.

2 Nondimensionalization of the Duffing equation

The nonautonomous ordinary differential equation having the following form

$$\ddot{x}+\xi\dot{x}+f(x)=F\cos\omega t, \tag{2}$$

where $f(x)$ is nonlinear, occurs in various physical problems. For example, the oscillation of a mass attached to an elastic spring, and excited by an external force, is governed by Eq. (2). In particular, the elastic spring has the restoring force $f(x)=x+\beta x^3$, where β is positive or negative corresponding to hard and soft spring restoration, respectively.

Very little generality is lost by choosing for the restoring force $f(x)$ with the following cubic form in x: $f(x)=\alpha x+\beta x^3$ $(\alpha>0)$. Thus, Eq. (2) becomes

$$\ddot{x}+\xi\dot{x}+\alpha x+\beta x^3=F\cos\omega t. \tag{3}$$

In Eq. (3), ξ is the damping parameter, $\sqrt{\alpha}$ is the natural frequency (denoted by ω_0) of the linear system, and β reflects the nonlinearity. By making the transformations

$$x^*=\frac{\alpha}{F}x,\ t^*=\sqrt{\alpha}t,\ \xi^*=\frac{\xi}{\sqrt{\alpha}},\ \beta^*=\frac{\beta F^2}{\alpha^3},\ \omega^*=\frac{\omega}{\sqrt{\alpha}}=\frac{\omega}{\omega_0},$$

Eq. (3) is transformed into:

$$\frac{d^2x^*}{dt^{*2}}+\xi^*\frac{dx^*}{dt^*}+x^*+\beta^*x^{*3}=\cos\omega^*t^*. \tag{4}$$

Therefore, ξ^*, ω^* and β^* are the control parameters except for the case where $\beta^* = \beta F^2/\alpha^3 = 0$. Specifically, $F = 0,\ \beta \neq 0$; $F \neq 0,\ \beta = 0$; and $F = 0,\ \beta = 0$ correspond to nonlinear free oscillation, linear forced oscillation and linear free oscillation, respectively. In order to distinguish the three types of possibilities, we investigate the Duffing equation having the following form:

$$\frac{d^2x^*}{dt^{*2}} + \xi^* \frac{dx^*}{dt^*} + x^* + \beta^* x^{*3} = F^* \cos \omega^* t^*. \tag{5}$$

For simplicity, all $*$ notation will be omitted in the remainder of this paper.

Note that ω^* in Eq. (5) is actually the ratio of the frequency of the impressed force ω to the natural frequency ω_0 of the linear system.

3 A simple algorithm for the collocation method applied in the time-domain, within a period of oscillation

In this section, we apply the collocation method in the time domain within a period of oscillation, for the periodic solutions of both harmonic and subharmonic oscillations, for the Duffing equation:

$$\ddot{x} + \xi \dot{x} + x + \beta x^3 = F \cos \omega t. \tag{6}$$

The harmonic solution of Eq. (6) is sought in the form:

$$x(t) = A_0 + \sum_{n=1}^{N} A_n \cos n\omega t + B_n \sin n\omega t. \tag{7}$$

The assumed form of $x(t)$ can be simplified by considering the symmetrical property of the nonlinear restoring force. First, Hayashi (1953c) pointed out that under circumstances when the nonlinearity is symmetric, i.e. $f(x)$ is odd in x, A_0 can be discarded. Second, it was demonstrated by Urabe (1969) both numerically and theoretically that the even harmonic components in Eq. (7) are zero. The approximate solution is simplified to:

$$x(t) = \sum_{n=1}^{N} A_n \cos (2n-1)\omega t + B_n \sin (2n-1)\omega t, \tag{8}$$

where N is the number of harmonics used in the desired approximation. $x(t)$ in Eq. (8) is called the N harmonic approximation (*or labeled as the N-th order approximation in the present paper*) of the harmonic solution.

In using the collocation method in the time domain, within a period of oscillation, we obtain the residual-error function $R(t)$ by substituting the approximate solution, Eq. (8), into the following equation:

$$R(t) = \ddot{x} + \xi\dot{x} + x + \beta x^3 - F\cos\omega t \neq 0. \tag{9}$$

Upon enforcing $R(t)$ to be zero at $2N$ equidistant points t_j over the domain $[0,\ 2\pi/\omega]$, we obtain a system of $2N$ nonlinear algebraic equations:

$$R_j(A_1, A_2, \ldots, A_N; B_1, B_2, \ldots, B_N) := \ddot{x}(t_j) + \xi\dot{x}(t_j) + x(t_j) + \beta x^3(t_j) - F\cos\omega t_j = 0_j, \tag{10}$$

where

$$x(t_j) = \sum_{n=1}^{N} A_n \cos(2n-1)\omega t_j + B_n \sin(2n-1)\omega t_j, \tag{11a}$$

$$\dot{x}(t_j) = \sum_{n=1}^{N} -(2n-1)\omega A_n \sin(2n-1)\omega t_j + (2n-1)\omega B_n \cos(2n-1)\omega t_j, \tag{11b}$$

$$\ddot{x}(t_j) = \sum_{n=1}^{N} -(2n-1)^2\omega^2 A_n \cos(2n-1)\omega t_j - (2n-1)^2\omega^2 B_n \sin(2n-1)\omega t_j, \tag{11c}$$

where j is an index value ranging from 1 to $2N$. Eq. (10) is the collocation-resulting system of NAEs for the harmonic solution.

Finally, the coefficients in Eq. (10) can be solved by nonlinear algebraic equations (NAEs) solvers, e.g, the Newton-Raphson method and the Jacobian matrix inverse-free algorithms [Dai, Paik, and Atluri (2011a,b); Liu, Dai, and Atluri (2011a,b)]. In this study, the more familiar Newton-Raphson method is employed. We emphasize that the Jacobian matrix **B** of Eq. (10) can be readily derived upon differentiating R_j with respect to A_i and B_i.

$$\mathbf{B} = [\frac{\partial R_j}{\partial A_i},\ \frac{\partial R_j}{\partial B_i}]_{2N\times 2N}, \tag{12}$$

where

$$\frac{\partial R_j}{\partial A_i} = -(2i-1)^2\omega^2\cos(2i-1)\omega t_j - \xi(2i-1)\omega\sin(2i-1)\omega t_j + \cos(2i-1)\omega t + 3\beta x^2(t_j)\cos(2i-1)\omega t$$

$$\frac{\partial R_j}{\partial B_i} = -(2i-1)^2\omega^2\sin(2i-1)\omega t_j + \xi(2i-1)\omega\cos(2i-1)\omega t_j + \sin(2i-1)\omega t + 3\beta x^2(t_j)\sin(2i-1)\omega t.$$

In order to capture the subharmonic behavior, a different approximate solution must be defined. Similarly, the N-th order approximation of the $1/3$ subharmonic solution can be assumed as

$$x(t) = \sum_{n=1}^{N} a_n \cos\frac{1}{3}(2n-1)\omega t + b_n \sin\frac{1}{3}(2n-1)\omega t. \tag{13}$$

After collocation, the resulting NAEs are

$$R_j(a_1, a_2, \ldots, a_N; b_1, b_2, \ldots, b_N) := \ddot{x}(t_j) + \xi\dot{x}(t_j) + x(t_j) + \beta x^3(t_j) - F\cos\omega t_j = 0_j, \tag{14}$$

where $j = 1, \ldots, 2N$. Eq. (14) is the collocation-resulting system of NAEs for the 1/3 subharmonic solutions. *A critical difference now, to capture the subharmonic solutions, is that the collocation should be performed over* $[0,\ 6\pi/\omega]$*, since the* $1/3$ *subharmonic solution has a period which is three times that of the harmonic solution.* The collocation-resulting NAEs may then be solved as above.

4 The relationship between the present collocation method and the high dimensional harmonic balance method (HDHB)

In this section, we explore the relation between the present simple collocation method and the High Dimensional Harmonic Balance method (HDHB) to give a better understanding of the HDHB.

For comparison, we choose the same model as in [Liu, Dowell, Thomas, Attar, and Hall (2006)] as follows:

$$m\ddot{x} + d\dot{x} + kx + \alpha x^3 = F\sin\omega t. \tag{15}$$

All the parameters in the above Duffing equation are kept in order to identify the source of the terms in the NAEs.

4.1 Harmonic balance method (HB)

Traditionally, to employ the standard harmonic balance method (HB), the solution of x is sought in the form of a truncated Fourier series expansion:

$$x(t) = x_0 + \sum_{n=1}^{N} \left[x_{2n-1}\cos n\omega t + x_{2n}\sin n\omega t\right], \tag{16}$$

where N is the number of harmonics used in the truncated Fourier series, and x_n, $n = 0, 1, \ldots, 2N$ are the unknown coefficients to be determined in the HB method.

We differentiate $x(t)$ with respect to t, leading to

$$\dot{x}(t) = \sum_{n=1}^{N} \left[-n\omega x_{2n-1} \sin n\omega t + n\omega x_{2n} \cos n\omega t\right], \tag{17a}$$

$$\ddot{x}(t) = \sum_{n=1}^{N} \left[-(n\omega)^2 x_{2n-1} \cos n\omega t - (n\omega)^2 x_{2n} \sin n\omega t\right]. \tag{17b}$$

Considering the cubic nonlinearity in Eq. (15), the nonlinear term can be expressed in terms of the truncated Fourier series with $3N$ harmonics:

$$x^3(t) = r_0 + \sum_{n=1}^{3N} \left[r_{2n-1} \cos n\omega t + r_{2n} \sin n\omega t\right]. \tag{18}$$

The $r_0,\ r_1,\ \ldots, r_{6N}$ are obtained by the following formulas:

$$r_0 = \frac{1}{2\pi} \int_0^{2\pi} \{x_0 + \sum_{k=1}^{N} \left[x_{2k-1} \cos k\theta + x_{2k} \sin k\theta\right]\}^3 d\theta, \tag{19a}$$

$$r_{2n-1} = \frac{1}{\pi} \int_0^{2\pi} \{x_0 + \sum_{k=1}^{N} \left[x_{2k-1} \cos k\theta + x_{2k} \sin k\theta\right]\}^3 \cos n\theta d\theta, \tag{19b}$$

$$r_{2n} = \frac{1}{\pi} \int_0^{2\pi} \{x_0 + \sum_{k=1}^{N} \left[x_{2k-1} \cos k\theta + x_{2k} \sin k\theta\right]\}^3 \sin n\theta d\theta. \tag{19c}$$

where $n = 1, 2, \ldots, 3N$, $\theta = \omega t$, and k is a dummy index.

In the harmonic balance method, one should balance the harmonics $1,\ \cos n\omega t$, $\sin n\omega t$, $n = 1, 2, \ldots, N$ to obtain the simultaneous $2N+1$ nonlinear algebraic equations. All the higher order harmonics $[n \geq N+1]$ in the nonlinear term are omitted. Thus, only the first N harmonics are retained, that is

$$x_{HB}^3(t) = r_0 + \sum_{n=1}^{N} \left[r_{2n-1} \cos n\omega t + r_{2n} \sin n\omega t\right]. \tag{20}$$

Therefore, only $r_0,\ r_1, \ldots,\ r_{2N}$ are needed in the harmonic balance method.

Next, substituting Eqs. (16)-(17b) and (20) into Eq. (15), and collecting the terms associated with each harmonic $1, \cos n\theta, \sin n\theta,\ n = 1, \ldots, N$, we finally obtain a system of NAEs in a vector form:

$$(m\omega^2 \mathbf{A}^2 + d\omega \mathbf{A} + k\mathbf{I})\mathbf{Q}_x + \alpha \mathbf{R}_x = F\mathbf{H}, \tag{21}$$

where $\mathbf{I}$ is a $2N+1$ dimension identity matrix, and

$$\mathbf{Q}_x = \begin{bmatrix} x_0 \\ x_1 \\ \vdots \\ x_{2N} \end{bmatrix}, \quad \mathbf{R}_x = \begin{bmatrix} r_0 \\ r_1 \\ \vdots \\ r_{2N} \end{bmatrix}, \quad \mathbf{H} = \begin{bmatrix} 0 \\ 0 \\ 1 \\ 0 \\ \vdots \\ 0 \end{bmatrix},$$

$$\mathbf{A} = \begin{bmatrix} 0 & 0 & 0 & \cdots & 0 \\ 0 & \mathbf{J}_1 & 0 & \cdots & 0 \\ 0 & 0 & \mathbf{J}_2 & \cdots & 0 \\ \vdots & \vdots & \vdots & \ddots & \vdots \\ 0 & 0 & 0 & \cdots & \mathbf{J}_N \end{bmatrix}, \quad \mathbf{J}_n = n \begin{bmatrix} 0 & \omega \\ -\omega & 0 \end{bmatrix}.$$

One should note that $r_n,\ n = 0, 1, \ldots, 2N$ are analytically expressed in terms of the coefficients $x_n,\ n = 0, 1, \ldots, 2N$, which makes the HB algebraically expensive for application. If many harmonics or complicated nonlinearity, i.e. more complicated than the cubic nonlinearity, are considered, the expressions for the nonlinear terms, Eqs. (19) become much more complicated.

4.2 HDHB

In order to eliminate needs for analytical expressions arising from the nonlinear term of the standard harmonic balance method, Thomas, Dowell, and Hall (2002); Hall, Thomas, and Clark (2002) developed the high dimensional harmonic balance method (HDHB). The key aspect is that instead of working in terms of Fourier coefficient variables x_n as in the HB method, the coefficient variables are instead recast in the time domain and stored at $2N+1$ equally spaced sub-time levels $x(t_i)$ over a period of one cycle of motion. The objective of the HDHB is to express the $\mathbf{Q}_x,\ \mathbf{R}_x$ in x_n [See Eq.(21)] by $\tilde{\mathbf{Q}}_x$, $\tilde{\mathbf{R}}_x$ in $x(t_n)$.

In the HDHB, the $2N+1$ harmonic balance Fourier coefficient solution variables are related to the time domain solution at $2N+1$ equally spaced sub-time levels over a period of oscillation via a constant Fourier transformation matrix. That is

$$\mathbf{Q}_x = \mathbf{E}\tilde{\mathbf{Q}}_x \tag{22}$$

where

$$\tilde{\mathbf{Q}}_x = \begin{bmatrix} x(t_0) \\ x(t_1) \\ x(t_2) \\ \vdots \\ x(t_{2N}) \end{bmatrix}, \quad \mathbf{Q}_x = \begin{bmatrix} x_0 \\ x_1 \\ x_2 \\ \vdots \\ x_{2N} \end{bmatrix}, \tag{23}$$

with $t_i = \frac{2\pi i}{(2N+1)\omega}$ $(i = 0,\ 1,\ 2\ldots,\ 2N)$, and the transform matrix is

$$\mathbf{E} = \frac{2}{2N+1} \begin{bmatrix} \frac{1}{2} & \frac{1}{2} & \ldots & \frac{1}{2} \\ \cos\theta_0 & \cos\theta_1 & \ldots & \cos\theta_{2N} \\ \sin\theta_0 & \sin\theta_1 & \ldots & \sin\theta_{2N} \\ \cos 2\theta_0 & \cos 2\theta_1 & \ldots & \cos 2\theta_{2N} \\ \sin 2\theta_0 & \sin 2\theta_1 & \ldots & \sin 2\theta_{2N} \\ \vdots & \vdots & \ddots & \vdots \\ \cos N\theta_0 & \cos N\theta_1 & \ldots & \cos N\theta_{2N} \\ \sin N\theta_0 & \sin N\theta_1 & \ldots & \sin N\theta_{2N} \end{bmatrix} \tag{24}$$

where $\theta_i = \omega t_i = \frac{2\pi i}{2N+1}$ $(i = 0,\ 1,\ 2\ldots,\ 2N)$. One should note that θ_i is the corresponding phase point of t_i.

Furthermore, the time domain solutions at the $2N+1$ equally spaced sub-time levels can be expressed in terms of the harmonic balance Fourier coefficient solution using the inverse of the Fourier transformation matrix, i.e.

$$\tilde{\mathbf{Q}}_x = \mathbf{E}^{-1}\mathbf{Q}_x, \tag{25}$$

where

$$\mathbf{E}^{-1} = \begin{bmatrix} 1 & \cos\theta_0 & \sin\theta_0 & \ldots & \cos N\theta_0 & \sin N\theta_0 \\ 1 & \cos\theta_1 & \sin\theta_1 & \ldots & \cos N\theta_1 & \sin N\theta_1 \\ \vdots & \vdots & \vdots & \vdots & \ddots & \vdots \\ 1 & \cos\theta_{2N} & \sin\theta_{2N} & \ldots & \cos N\theta_{2N} & \sin N\theta_{2N} \end{bmatrix}. \tag{26}$$

Similarly, $\mathbf{H} = \mathbf{E}\tilde{\mathbf{H}}$, where

$$\tilde{\mathbf{H}} = \begin{bmatrix} \sin\theta_0 \\ \sin\theta_1 \\ \vdots \\ \sin\theta_{2N} \end{bmatrix}. \tag{27}$$

So far, $\mathbf{Q}_x$ and $\mathbf{H}$ have been transformed by the transformation matrix. Now, we turn to process the nonlinear term $\mathbf{R}_x$. We define the $\tilde{\mathbf{R}}_x$ as

$$\tilde{\mathbf{R}}_x = \begin{bmatrix} x^3(t_0) \\ x^3(t_1) \\ \vdots \\ x^3(t_{2N}) \end{bmatrix}. \tag{28}$$

In the studies by Thomas, Dowell, and Hall (2002); Hall, Thomas, and Clark (2002); Liu, Dowell, Thomas, Attar, and Hall (2006), they use the relation $\mathbf{R}_x = \mathbf{E}\tilde{\mathbf{R}}_x$ without further discussion. However, this relation is not strictly true, as seen below.

We consider the relation between $\mathbf{E}^{-1}\mathbf{R}_x$ and $\tilde{\mathbf{R}}_x$ instead.

$$\begin{aligned}
\mathbf{E}^{-1}\mathbf{R}_x = & \begin{bmatrix} 1 & \cos\theta_0 & \sin\theta_0 & \dots & \cos N\theta_0 & \sin N\theta_0 \\ 1 & \cos\theta_1 & \sin\theta_1 & \dots & \cos N\theta_1 & \sin N\theta_1 \\ \vdots & \vdots & \vdots & \ddots & \vdots & \vdots \\ 1 & \cos\theta_{2N} & \sin\theta_{2N} & \dots & \cos N\theta_{2N} & \sin N\theta_{2N} \end{bmatrix} \begin{bmatrix} r_0 \\ r_1 \\ \vdots \\ r_{2N} \end{bmatrix} \\
= & \begin{bmatrix} r_0 + \sum_{n=1}^{N} [r_{2n-1}\cos n\theta_0 + r_{2n}\sin n\theta_0] \\ r_0 + \sum_{n=1}^{N} [r_{2n-1}\cos n\theta_1 + r_{2n}\sin n\theta_1] \\ \vdots \\ r_0 + \sum_{n=1}^{N} [r_{2n-1}\cos n\theta_{2N} + r_{2n}\sin n\theta_{2N}] \end{bmatrix} \\
= & \begin{bmatrix} x^3_{HB}(t_0) \\ x^3_{HB}(t_1) \\ \vdots \\ x^3_{HB}(t_{2N}) \end{bmatrix}
\end{aligned}$$

Considering Eq. (18),

$$\tilde{\mathbf{R}}_x = \begin{bmatrix} x^3(t_0) \\ x^3(t_1) \\ \vdots \\ x^3(t_{2N}) \end{bmatrix} = \begin{bmatrix} r_0 + \sum_{n=1}^{3N} [r_{2n-1}\cos n\theta_0 + r_{2n}\sin n\theta_0] \\ r_0 + \sum_{n=1}^{3N} [r_{2n-1}\cos n\theta_1 + r_{2n}\sin n\theta_1] \\ \vdots \\ r_0 + \sum_{n=1}^{3N} [r_{2n-1}\cos n\theta_{2N} + r_{2n}\sin n\theta_{2N}] \end{bmatrix}$$

It is clear that $\mathbf{E}^{-1}\mathbf{R}_x$ and $\tilde{\mathbf{R}}_x$ are not equal.

Once the approximate relation: $\mathbf{E}^{-1}\mathbf{R}_x = \tilde{\mathbf{R}}_x$ is applied, using $\mathbf{Q}_x = \mathbf{E}\tilde{\mathbf{Q}}_x$, $\mathbf{H}_x = \mathbf{E}\tilde{\mathbf{H}}_x$, Eq. (21) is then rewritten as

$$(m\omega^2\mathbf{A}^2 + d\omega\mathbf{A} + k\mathbf{I})\mathbf{E}\tilde{\mathbf{Q}}_x + \alpha\mathbf{E}\tilde{\mathbf{R}}_x = F\mathbf{E}\tilde{\mathbf{H}}. \tag{29}$$

It is seen that by using the approximation $\mathbf{R}_x = \mathbf{E}^{-1}\tilde{\mathbf{R}}_x$ in Eq. (29), the HDHB absorbs the higher harmonics in the nonlinear term $\tilde{\mathbf{R}}_x$. This may be one source of non-physical solutions generated by the HDHB method.

Multiplying both sides of the above equation by $\mathbf{E}^{-1}$ yields:

$$(m\omega^2\mathbf{D}^2 + d\omega\mathbf{D} + k\mathbf{I})\tilde{\mathbf{Q}}_x + \alpha\tilde{\mathbf{R}}_x = F\tilde{\mathbf{H}}, \tag{30}$$

where $\mathbf{D} = \mathbf{E}^{-1}\mathbf{A}\mathbf{E}$. The Eq. (30) is referred to as the HDHB solution system.

We emphasize that the HDHB is distinct from the harmonic balance method only in the nonlinear term, where the HDHB includes higher order harmonic terms ($n = N+1, \ldots, 3N$).

In this section, the HDHB is derived based on a approximation from the standard harmonic balance method. The HDHB and the harmonic balance method are not equivalent. *Interestingly, the HDHB can be derived strictly from the point collocation method presented in Section 3.*

4.3 Equivalence between the HDHB and the collocation method

Herein, we derive the HDHB from the collocation method to demonstrate their equivalence. In Section 3, the Duffing equation and the trial function used are not uniform to those in this section. Thus, we need to reformulate the collocation method herein. Using the approximate solution, Eq. (16), we first write the residual-error function of the Eq. (15) as:

$$R(t) = m\ddot{x} + d\dot{x} + kx + \alpha x^3 - F\sin\omega t \neq 0. \tag{31}$$

Upon enforcing $R(t)$ to be zero at $2N+1$ equidistant points t_i over the domain $[0,\ 2\pi/\omega]$, we obtain a system of $2N+1$ nonlinear algebraic equations:

$$R_i(x_0, x_1, \ldots, x_{2N}) := m\ddot{x}(t_i) + d\dot{x}(t_i) + kx(t_i) + \alpha x^3(t_i) - F\sin\omega t_i = 0_i. \tag{32}$$

Later on, we explain the time domain transformation or the Fourier transformation in the view of collocation. Now, we consider each term in the above equation separately.

For comparison, the trial solution of the collocation method is the same as in Eq. (16). Collocating $x(t)$ in Eq. (16) at points t_i, we have

$$x(t_i) = x_0 + \sum_{n=1}^{N} \left[x_{2n-1}\cos n\omega t_i + x_{2n}\sin n\omega t_i\right]. \tag{33}$$

Considering $\theta_i = \omega t_i$, Eq. (33) can be rewritten in a matrix form

$$\begin{bmatrix} x(t_0) \\ x(t_1) \\ \vdots \\ x(t_{2N}) \end{bmatrix} = \begin{bmatrix} 1 & \cos\theta_0 & \sin\theta_0 & \dots & \cos N\theta_0 & \sin N\theta_0 \\ 1 & \cos\theta_1 & \sin\theta_1 & \dots & \cos N\theta_1 & \sin N\theta_1 \\ \vdots & \vdots & \vdots & \ddots & \vdots & \vdots \\ 1 & \cos\theta_{2N} & \sin\theta_{2N} & \dots & \cos N\theta_{2N} & \sin N\theta_{2N} \end{bmatrix} \begin{bmatrix} x_0 \\ x_1 \\ \vdots \\ x_{2N} \end{bmatrix}. \tag{34}$$

Therefore

$$\tilde{\mathbf{Q}}_x = \begin{bmatrix} x(t_0) \\ x(t_1) \\ \vdots \\ x(t_{2N}) \end{bmatrix} = \mathbf{E}^{-1}\mathbf{Q}_x. \tag{35}$$

In comparison with Eq. (25), we see that the Fourier transformation matrix $\mathbf{E}$ can be interpreted as the collocation-resulting matrix in Eq. (34).

Similarly, collocating $\dot{x}(t)$ at $2N+1$ equidistant time points t_i, we have

$$\dot{x}(t_i) = \sum_{n=1}^{N} \left[-n\omega x_{2n-1} \sin n\omega t_i + n\omega x_{2n} \cos n\omega t_i \right]. \tag{36}$$

The above equation can be written in a matrix form:

$$\begin{bmatrix} \dot{x}(t_0) \\ \dot{x}(t_1) \\ \vdots \\ \dot{x}(t_{2N}) \end{bmatrix} = \omega \begin{bmatrix} 0 & -\sin\theta_0 & \cos\theta_0 & \dots & -N\sin N\theta_0 & N\cos N\theta_0 \\ 0 & -\sin\theta_1 & \cos\theta_1 & \dots & -N\sin N\theta_1 & N\cos N\theta_1 \\ \vdots & \vdots & \vdots & \ddots & \vdots & \vdots \\ 0 & -\sin\theta_{2N} & \cos\theta_{2N} & \dots & -N\sin N\theta_{2N} & N\cos N\theta_{2N} \end{bmatrix} \begin{bmatrix} x_0 \\ x_1 \\ \vdots \\ x_{2N} \end{bmatrix}. \tag{37}$$

We observe that the square matrix in the above equation can be expressed by two

existing matrices:

$$\begin{bmatrix} 0 & -\sin\theta_0 & \cos\theta_0 & \dots & -N\sin N\theta_0 & N\cos N\theta_0 \\ 0 & -\sin\theta_1 & \cos\theta_1 & \dots & -N\sin N\theta_1 & N\cos N\theta_1 \\ \vdots & \vdots & \vdots & \ddots & \vdots & \vdots \\ 0 & -\sin\theta_{2N} & \cos\theta_{2N} & \dots & -N\sin N\theta_{2N} & N\cos N\theta_{2N} \end{bmatrix}$$

$$= \begin{bmatrix} 1 & \cos\theta_0 & \sin\theta_0 & \dots & \cos N\theta_0 & \sin N\theta_0 \\ 1 & \cos\theta_1 & \sin\theta_1 & \dots & \cos N\theta_1 & \sin N\theta_1 \\ \vdots & \vdots & \vdots & \ddots & \vdots & \vdots \\ 1 & \cos\theta_{2N} & \sin\theta_{2N} & \dots & \cos N\theta_{2N} & \sin N\theta_{2N} \end{bmatrix} \begin{bmatrix} 0 & 0 & 0 & \cdots & 0 \\ 0 & \mathbf{J}_1 & 0 & \cdots & 0 \\ 0 & 0 & \mathbf{J}_2 & \cdots & 0 \\ \vdots & \vdots & \ddots & \cdots & \vdots \\ 0 & 0 & 0 & \cdots & \mathbf{J}_N \end{bmatrix}$$

$$= \mathbf{E}^{-1}\mathbf{A}.$$

Thus, we have

$$\begin{bmatrix} \dot{x}(t_0) \\ \dot{x}(t_1) \\ \vdots \\ \dot{x}(t_{2N}) \end{bmatrix} = \omega\mathbf{E}^{-1}\mathbf{A}\mathbf{Q}_x. \tag{38}$$

In the same manner, collocating $\ddot{x}(t)$ at $2N+1$ equidistant time points t_i, we have

$$\ddot{x}(t_i) = \sum_{n=1}^{N} \left[-n^2\omega^2 x_{2n-1}\cos n\omega t_i - n^2\omega^2 x_{2n}\sin n\omega t_i \right]. \tag{39}$$

Eq. (39) is written in a matrix form:

$$\begin{bmatrix} \ddot{x}(t_0) \\ \ddot{x}(t_1) \\ \vdots \\ \ddot{x}(t_{2N}) \end{bmatrix} =$$

$$\omega^2 \begin{bmatrix} 0 & -\cos\theta_0 & -\sin\theta_0 & \dots & -N^2\cos N\theta_0 & -N^2\sin N\theta_0 \\ 0 & -\cos\theta_1 & -\sin\theta_1 & \dots & -N^2\cos N\theta_1 & -N^2\sin N\theta_1 \\ \vdots & \vdots & \vdots & \ddots & \vdots & \vdots \\ 0 & -\cos\theta_{2N} & -\sin\theta_{2N} & \dots & -N^2\cos N\theta_{2N} & -N^2\sin N\theta_{2N} \end{bmatrix} \begin{bmatrix} x_0 \\ x_1 \\ \vdots \\ x_{2N} \end{bmatrix}. \tag{40}$$

Note that the square matrix in the above equation is equal to $\mathbf{E}^{-1}\mathbf{A}^2$. Therefore,

$$\begin{bmatrix} \ddot{x}(t_0) \\ \ddot{x}(t_1) \\ \vdots \\ \ddot{x}(t_{2N}) \end{bmatrix} = \omega^2 \mathbf{E}^{-1}\mathbf{A}^2 \mathbf{Q}_x. \tag{41}$$

Now, substituting Eqs. (35,38,41) and Eq. (28) into the collocation-resulting algebraic Eq. (32), we obtain:

$$\mathbf{E}^{-1}\left(m\omega^2\mathbf{A}^2 + d\omega\mathbf{A} + k\mathbf{I}\right)\mathbf{Q}_x + \alpha\tilde{\mathbf{R}}_x = F\tilde{\mathbf{H}}. \tag{42}$$

By using Eq. (35), i.e. $\mathbf{Q}_x = \mathbf{E}\tilde{\mathbf{Q}}_x$, the above equation can be written as

$$\left(m\omega^2\mathbf{D}^2 + d\omega\mathbf{D} + k\mathbf{I}\right)\tilde{\mathbf{Q}}_x + \alpha\tilde{\mathbf{R}}_x = F\tilde{\mathbf{H}}. \tag{43}$$

Eq. (43) is the transformed collocation system. No approximation is adopted during the derivation. We see that Eq. (43) is the same as Eq. (30). *Therefore, we have demonstrated the equivalence of the collocation method and the high dimensional harmonic balance method (HDHB). We come to the conclusion that the HDHB approach is no more than a cumbersome version of the presently proposed simple collocation method.*

In summary: (a) The collocation method is simpler. It does not call for the Fourier transformation and works in terms of Fourier coefficient variables. Section 3 shows that the collocation algebraic system and its Jacobian matrix can be obtained easily without intense symbolic operation. (b) The HDHB is a transformed collocation method. It can be derived from the collocation method rigorously.

The reason for the occurrence of the non-physical solution by HDHB can be understood by treating it as a collocation method. In the previous studies, they were not aware of the fact that the HDHB is essentially a collocation method. Thus, they mostly compare the the HDHB1[1] or HDHB2 with HB1 and HB2. As is known that the harmonic balance method (time Galerkin method) works relatively well with few harmonics. As the number N of the harmonics is increased in the trial solution, Eq. (16), it may not be sufficient to collocate the residual-error, Eq. (31), only at $2N+1$ points in a period [See Atluri (2005)]. One may have to use M collocation points, $M > 2N+1$, to obtain a reasonable solution. As $M \to \infty$ one may develop a method of least-squared error, wherein one seeks to minimize $\int_0^T R^2(t)dt$ [T is the period of the periodic solution] with respect to the coefficients x_n, $(n = 0, 1, \ldots, 2N)$ of Eq. (16). This will be pursued in a future study.

[1] HDHB1 means HDHB with one harmonic.

5 Initial values for the Newton-Raphson method

In Section 3, the collocation method has been formulated. The algebraic systems arising from the harmonic oscillation and $1/3$ subharmonic oscillation are given in Eq. (10) and (14), respectively. In order to solve the resulting NAEs, one has to give initial values for the Newton iterative process to start. It is known that the system has multiple solutions, viz, multiple steady states. Hence it is expected to provide the deterministic initial values to direct the solutions to the system of NAEs to the desired solution. In this section, we provide the initial values for the higher harmonic approximation. The initial values for undamped and damped systems are considered separately.

5.1 Initial values for the NAE system, for undamped Duffing oscillator

In this subsection, we consider the undamped system:

$$\ddot{x}+x+\beta x^3 = F\cos\omega t. \tag{44}$$

5.1.1 Initial values for the iterative solution of NAEs for capturing the $1/3$ *subharmonic solution of the undamped system*

In the case of undamped system, the trial function in Eq. (13) can be simplified further. All the sine terms turn out to be zero in the course of the calculation. This is because the damping is absent. Further rigorous demonstrations can be found in Stoker (1950), Urabe (1965, 1969) and Urabe and Reiter (1966). For brevity, we therefore omit the sines at the onset and seek the subharmonic solution in the following form

$$x(t) = \sum_{n=1}^{N} a_n \cos\frac{1}{3}(2n-1)\omega t. \tag{45}$$

To find the starting values for the Newton iterative process, we simply consider the approximation with $N = 2$:

$$x(t) = a_1^{(2)}\cos\frac{1}{3}\omega t + a_2^{(2)}\cos\omega t. \tag{46}$$

The superscript (2) is introduced, on one hand, to distinguish from the coefficients a_1, a_2 in the N-th order approximation in Eq. (45), and on the other hand to denote the order of harmonic approximation. For brevity, however, we omit the superscript unless needed.

Substitution of Eq. (46) in Eq. (44) and equating the coefficients of $\cos 1/3\omega t$ and $\cos \omega t$, leads to two simultaneous nonlinear algebraic equations

$$\begin{cases} a_1 \left[36 - 4\omega^2 + 27(a_1^2 + a_1 a_2 + 2a_2^2)\beta\right] = 0 & \text{(47a)} \\ (a_1^3 + 6a_1^2 a_2 + 3a_2^3)\beta + 4a_2(1-\omega^2) - 4F = 0. & \text{(47b)} \end{cases}$$

From the Eq. (47a), we have two possibilities:

$$a_1 = 0 \;\; or \;\; 36 - 4\omega^2 + 27(a_1^2 + a_1 a_2 + 2a_2^2)\beta = 0.$$

Each possibility leads Eqs. (47) to a different system:

$$\begin{cases} a_1 = 0 & \text{(48a)} \\ 3a_2^3\beta + 4a_2(1-\omega^2) = 4F \qquad \text{from Eq. (47b)} & \text{(48b)} \end{cases}$$

and

$$\begin{cases} \omega^2 = 9 + \dfrac{27}{4}(a_1^2 + a_1 a_2 + 2a_2^2)\beta & \text{(49a)} \\ (a_1^3 + 6a_1^2 a_2 + 3a_2^3)\beta + 4a_2(1-\omega^2) = 4F. & \text{(49b)} \end{cases}$$

We can see that a_2 in Eq. (48b) actually reduces to $A_1^{(1)}$ [see Eq. (8)], since $1/3$ subharmonic component is zero. Similar to the definition of lower-case letter, the capital A_1 coefficient is in reference to Eq. (8) where the subharmonics are not yet included in the trial function. The superscript (1) denotes the order of approximation.

For a hard spring system, i.e. $\beta > 0$, it can be immediately seen from Eq. (49a) that the frequency ω of the impressed force must be greater than 3 to ensure the existence of real roots for Eqs. (49). Here 3 refers to three times the natural frequency of the linear system. The natural frequency of the linear system is scaled to unity in Eq. (5).

To initialize the Newton iterative process, we compute the second order approximation as the initial values of the N-th order approximation.

As stated above, we solve Eq. (49) to obtain coefficients of the second order subharmonic approximation. We set the initial values of the coefficients of the N-th order approximation in Eq. (45) as

$$a_1 = a_1^{(2)}, \;\; a_2 = a_2^{(2)}, \;\; a_3 = a_4 = \cdots = a_N = 0.$$

Starting from the initial values, we can solve the NAEs resulting from the application of collocation in the time domain within an appropriate period of the periodic solution, similar to Eq. (14), by the Newton-Raphson method.

It should be noted that there might be multiple sets of solutions for Eqs. (49) at a certain frequency. Each set of initial values, viz, the coefficients of the low order approximation, may direct the NAEs to its corresponding high order approximation as will be verified later.

5.1.2 *Initial values for the iterative solution of NAEs for capturing the harmonic solution of the undamped system*

Similar to the N-th order approximation of the $1/3$ subharmonic solution in Eq. (45), the N-th order approximation of the harmonic solution can be sought in the form

$$x(t) = \sum_{n=1}^{N} A_n \cos(2n-1)\omega t. \tag{50}$$

In Section 5.1.1, we have obtained Eqs. (48), which are the NAEs for the second order $1/3$ subharmonic solution. Since a_1 is 0, a_2 in Eq. (48b) actually turns out to be $A_1^{(1)}$. Therefore, the N-th order approximation can start by letting

$$A_1 = A_1^{(1)}, \;\; A_2 = A_3 = \cdots = A_N = 0. \tag{51}$$

The first order harmonic approximation is verified reasonably accurately in the example in Section 6. Once the initial values are obtained, we can solve the system of NAEs by Newton-Raphson method.

5.2 Initial values for the NAEs arising from the damped system

In Section 5.1, we provided initial values for the harmonic and subharmonic solutions of an undamped system. For Eq. (6) with small damping, i.e. $|\xi|$ is small, the solution is developed in Fourier series as Eq. (13) for $1/3$ subharmonic solution or Eq. (8) for harmonic solution. The N harmonic, i.e. N-th order, approximations of Eqs. (13) and (8) are supposed to be close to Eqs. (45) and (50); therefore, the initial values can be supplied by the low harmonic approximation of the undamped Duffing equation [Urabe (1969)].

However, this is not applicable to the system with a relatively large damping. On the one hand, one may ask how small should the damping be so as to be safe to use the undamped initial values. On the another hand, Urabe's scheme fails to provide reasonable initial values for a strongly damped system. In our scheme, we seek the initial values by solving the lowest two harmonic approximation.

5.2.1 Initial values for the iterative solution of NAEs for capturing the $1/3$ subharmonic solution of the damped system

We assume the second order $1/3$ subharmonic solution as follows

$$x(t) = a_1 \cos\frac{1}{3}\omega t + b_1 \sin\frac{1}{3}\omega t + a_2 \cos\omega t + b_2 \sin\omega t. \tag{52}$$

Substitution of Eq. (52) into the Duffing equation (6) as well as collecting the coefficients of $\cos\frac{1}{3}\omega t$, $\sin\frac{1}{3}\omega t$, $\cos\omega t$ and $\sin\omega t$, leads to a system of four simultaneous NAEs, which is given in Appendix A.

Hence, this system of simultaneous NAEs determines the coefficients of the second order $1/3$ subharmonic approximation. For any given problem [ξ, β, F and ω specified], no matter how strong the damping is, we can calculate the initial values by solving Eq. (59) in Appendix A. Multiple sets of solutions can be obtained easily by Mathematica. In a physical view, the multiple solutions correspond to various steady state motions.

Therefore, the N-th order approximation can start with

$$\begin{aligned}
&a_1 = a_1^{(2)}, \;\; b_1 = b_1^{(2)},\\
&a_2 = a_2^{(2)}, \;\; b_2 = b_2^{(2)},\\
&a_3 = a_4 = \cdots = a_N = 0,\\
&b_3 = b_4 = \cdots = b_N = 0.
\end{aligned}$$

Consequently, the system of $2N$ nonlinear algebraic equations in Eq. (14) is solved for the $1/3$ subharmonic solution.

5.2.2 Initial values for the iterative solution of NAEs for capturing the harmonic solution of the damped system

Similarly, the second order approximation for the harmonic oscillation is

$$x(t) = A_1 \cos\omega t + B_1 \sin\omega t + A_2 \cos 3\omega t + B_2 \sin 3\omega t. \tag{53}$$

Substitution of Eq. (53) into the Duffing equation (6) and then collecting coefficients of $\cos\omega t$, $\sin\omega t$, $\cos 3\omega t$ and $\sin 3\omega t$, leads to a system of NAEs in Appendix B.

This system of NAEs determines the coefficients of the second order approximation. Hence, the N-th order approximation can start with

$$\begin{aligned}
&A_1 = A_1^{(2)}, \;\; B_1 = B_1^{(2)},\\
&A_2 = A_2^{(2)}, \;\; B_2 = B_2^{(2)},\\
&A_3 = A_4 = \cdots = A_N = 0,\\
&B_3 = B_4 = \cdots = B_N = 0.
\end{aligned}$$

Consequently, the collocation-resulting NAEs can be solved. Then, we can obtain the N-th order harmonic solution after inserting the determined coefficients into trial function in Eq. (8).

6 Numerical example 1: Undamped Duffing equation

We apply the proposed method of collocation in the time domain, within a period of oscillation, to solve the undamped Duffing equation. Ludeke and Cornett (1966) studied the undamped Duffing equation having the form

$$\frac{d^2x}{d\tau^2} + 2x + 2x^3 = 10\cos\Omega\tau \tag{54}$$

with an analog computer. We solve this problem by the present scheme. Firstly, making a transformation:

$$\tau = \frac{t}{\sqrt{2}},\ \Omega = \sqrt{2}\omega,$$

we have

$$\ddot{x} + x + x^3 = 5\cos\omega t, \tag{55}$$

where $\dot{x}$ denotes dx/dt. For the harmonic solution, we solve Eq. (48) to obtain the first order approximation as the initial values for a specified ω_g. For the subharmonic solution, Eq. (49) is solved for the second order approximation.

We can sweep ω, starting from ω_g, back and forth to find the frequency response curve of the considered problem. Throughout the paper, the solution of the previous frequency is used as the initial values of its immediate subsequent frequency. Thus, the specified ω_g is named the generating frequency. It is not hard to choose a proper ω_g. We will illustrate this in the examples.

For the undamped case, we can plot the graphs of a_1 vs ω, a_2 vs ω and $A_1^{(1)}$ vs ω, which provide the information of the onset of the subharmonic oscillation, the bifurcation point and the pure subharmonic frequency. Fig. 1 shows the general pattern of the response curves. The the solid and dashed curves in Fig. 1(a) and Fig. 1(b) indicate which branch must be considered simultaneously. They also indicate the onset of the occurrence of the $1/3$ subharmonic response. $a_1 = 0$, viz, point A in Fig. 1(a) determines the bifurcation frequency. $a_2 = 0$, viz, point B in Fig. 1(b) is the frequency where the pure $1/3$ subharmonic oscillation occurs. Fig. 1(c) is the amplitude frequency response curve of the harmonic response of the first order approximation.

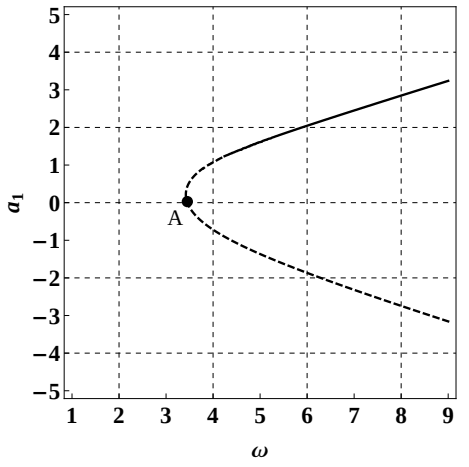

(a) a_1 *vs* ω

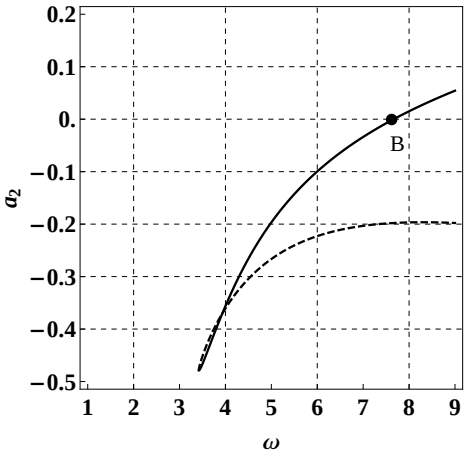

(b) a_2 *vs* ω

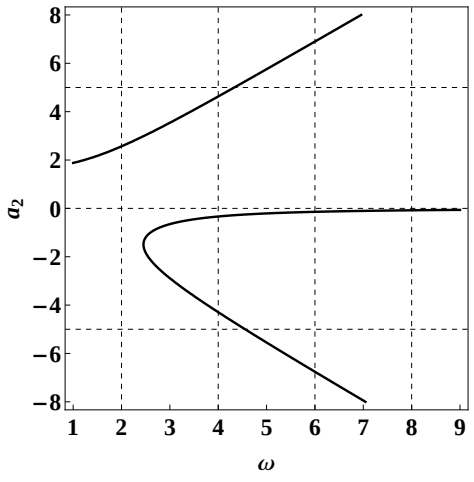

(c) a_2 *vs* ω

Figure 1: The second order approximation of $1/3$ subharmonic solution of the undamped Duffing equation: (a) $1/3$ subharmonic amplitude varying with frequency ω; (b) fundamental harmonic amplitude varying with frequency ω; (c) fundamental harmonic amplitude a_2 varying with frequency ω, in this case $a_1 = 0$, a_2 represents $A_1^{(1)}$.

Table 1: Initial values at $\omega_g = 4$

	$\cos 1/3\omega t$	$\cos \omega t$
SUBSOL1	-0.7194743839857893	-0.3605474805023799
SUBSOL2	1.0808818787916024	-0.3561553451108572
HARSOL1	0	4.630311850542268
HARSOL2	0	-4.295095097328164
HARSOL3	0	-0.3352167532141037

Table 2: Coefficients of the subharmonic solutions for $N = 8$, at $\omega_g = 4$

	SUBSOL1	SUBSOL2
$\cos 1/3\omega t$	-0.716782379738396	1.079100277428763
$\cos \omega t$	-0.360622588276577	-0.356287363474015
$\cos 5/3\omega t$	-0.004933880272422	-0.005011933668311
$\cos 7/3\omega t$	-0.000866908478371	0.001202617368613
$\cos 3\omega t$	-0.000100868293579	-0.000056982080267
$\cos 11/3\omega t$	-0.000004288223870	-0.000005549305123
$\cos 13/3\omega t$	-0.000000470514428	0.000000435376073
$\cos 5\omega t$	-0.000000038364455	0.000000006711708

Table 3: Coefficients of the harmonic solutions for $N = 12$, at $\omega_g = 4$

	HARSOL1	HARSOL2	HARSOL3
$\cos \omega t$	4.521893823447083	-4.205552387932138	-0.335217130152840
$\cos 3\omega t$	0.207195704577293	-0.160416386994274	-0.000065931786928
$\cos 5\omega t$	0.009041646033017	-0.005939980362846	-0.000000013934922
$\cos 7\omega t$	0.000395158065012	-0.000219574108227	-0.000000000002897
$\cos 9\omega t$	0.000017272530534	-0.000008115364584	-0.000000000000001
$\cos 11\omega t$	0.000000755010323	-0.000000299931252	-0.000000000000000
$\cos 13\omega t$	0.000000033002979	-0.000000011084898	0.000000000000000
$\cos 15\omega t$	0.000000001442629	-0.000000000409676	0.000000000000000
$\cos 17\omega t$	0.000000000063060	-0.000000000015141	0.000000000000000
$\cos 19\omega t$	0.000000000002757	-0.000000000000560	0.000000000000000
$\cos 21\omega t$	0.000000000000121	-0.000000000000021	0.000000000000000
$\cos 23\omega t$	0.000000000000005	-0.000000000000001	-0.000000000000000

In this case, we choose the generating frequency $\omega_g = 4$. It shows from Fig. 1(b)(c) that all five sets of solutions exist at ω_g. *This means we can find five steady state motions at a single generating frequency, by sweeping* ω *from where, we obtain all five branches.* The initial values from Eqs. (48) and (49) are listed in Table 1.

The comparison of the initial values in Table 1 with the high order solutions in Tables 2 and 3 confirm that the initial values are relatively close to the high order solutions. Essentially, the low order approximation and its corresponding N-th solution are qualitatively the same [on the same branch of the response curve]. In the tables, SUBSOL and HARSOL denote subharmonic solution and harmonic solution respectively.

Table 2 shows that the $1/3$ subharmonic and harmonic components dominate others, which illustrates the validity of using the second order approximation as the initials to its high order solution. Table 3 shows that the first harmonic is much larger than the higher order components, which also confirms the validity of applying $A_1^{(1)}$ as the initial value. *We can conclude by comparing Table 1 and 3 that the first, second and third columns of Table 3 correspond to the upper, unstable and lower branches*[2]*, respectively.*

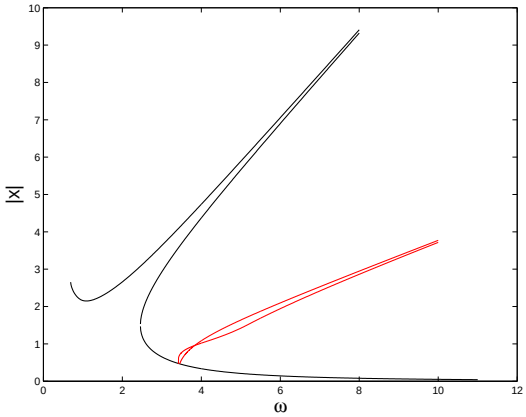

Figure 2: The peak amplitude $|x|$ versus frequency curve for the Duffing equation: $\ddot{x} + x + x^3 = 5\cos\omega t$; the black curve represents the harmonic response; the red curve represents the $1/3$ subharmonic response.

By sweeping ω back and forth, starting at ω_g, over all branches, we finally ob-

[2] The upper, unstable and lower branches are discussed in $|x|_{max}$ vs ω plane of the harmonic oscillation. Fig. 1(c) is actually a first order harmonic response: x_{max} vs ω, of the harmonic oscillation. The $|x|_{max}$, i.e. the peak amplitude of x, is denoted by $|x|$ in all figures.

tain the response curves for both harmonic and subharmonic oscillations. Fig. 2 plots the peak amplitude $|x|$ versus frequency curve. Both harmonic and subharmonic responses are provided. Unless otherwise specified, the stop criterion of the Newton-Raphson solver is $\varepsilon = 10^{-10}$ throughout the paper. Since damping is absent in the current problem, both harmonic and subharmonic responses will go to infinity with the increase of the impressed frequency.

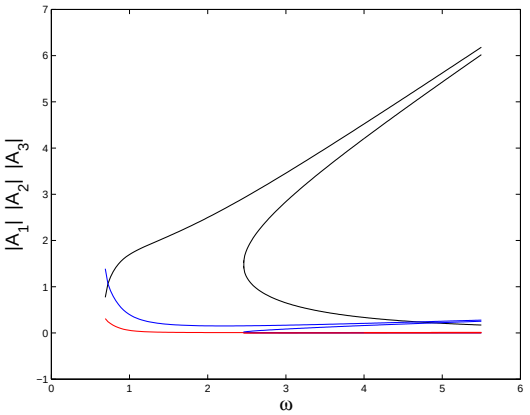

Figure 3: The harmonic amplitude versus frequency curves of the harmonic solution for the Duffing equation $\ddot{x}+x+x^3 = 5\cos\omega t$: the black curve represents the first harmonic amplitude $|A_1|$ versus ω; the blue curve represents the third harmonic amplitude $|A_2|$ versus ω; the red curve represents the fifth harmonic amplitude A_3 versus ω.

Fig. 3 provides the response curves of the harmonic solution. The amplitude of each harmonic is plotted. For the upper branch of $|A_1|$, i.e. the amplitude of the first harmonic. It dominates the oscillation from about $\omega = 1$ to infinity. The middle branch is an unstable one which is practically unrealizable. The third harmonic component is comparable with the lower branch of the first harmonic component at $\omega > 4$. It can be seen that the fifth component is very weak far away from $\omega < 1$. It should be noted that the third and fifth harmonics are significant where $\omega < 1$.

Fig. 4 provides the response curves of the subharmonic solution. The amplitudes of $1/3$, 1 and $5/3$ harmonic components are given. It indicates that the $5/3$ harmonic component is very weak compared with the $1/3$ and the first harmonic components. The subharmonic oscillation emerges from about $\omega = 3.5$, which agrees with the above statement that the $1/3$ subharmonic oscillation starts at the frequency being greater than three times of the natural frequency.

It indicates that the pure subharmonic oscillation may occur at the frequency where

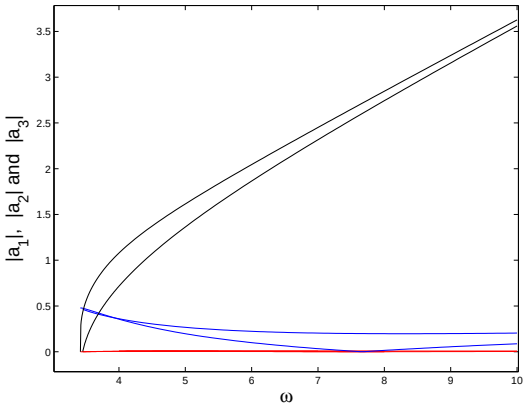

Figure 4: The harmonic amplitude versus frequency curves of the $1/3$ subharmonic solution for the Duffing equation $\ddot{x}+x+x^3=5\cos\omega t$: the black curve represents the $1/3$ subharmonic amplitude $|a_1|$ versus ω; the blue curve represents the harmonic amplitude $|a_2|$ versus ω; the red curve represents the $5/3$ ultrasubharmonic amplitude $|a_3|$ versus ω.

A_1 is zero. It is about $\omega=7.5$ from Fig. 4. This is also predicted by the second order approximation in Eq. (49) with $a_2=0$, ω as unknown, giving $\omega=7.66384$.

7 Numerical example 2: Damped Duffing equation

In this section, we investigate the effect of each parameter in the Duffing equation

$$\ddot{x}+\xi\dot{x}+x+\beta x^3=F\cos\omega t. \tag{56}$$

For doing so, we compute the amplitude frequency curves for various ξ, β and F. As before, we exclusively focus on the harmonic and $1/3$ subharmonic responses.

Eqs. (8) and (13) are the N-th order approximations to the harmonic and $1/3$ subharmonic solutions. Eqs. (60) and (59) are used to generate the initial values for the higher order approximations of harmonic and subharmonic solutions respectively. The generating frequency ω_g is chosen according to the considered case.

7.1 The effect of damping ξ

Fig. 5 gives the amplitude-frequency curves with various damping. It indicates that a smaller damping ξ stretches the response curve. The smaller the damping is, the longer the tip of the upper harmonic response and the subharmonic response will be. When $\xi=0$, the upper harmonic response and the subharmonic response go to

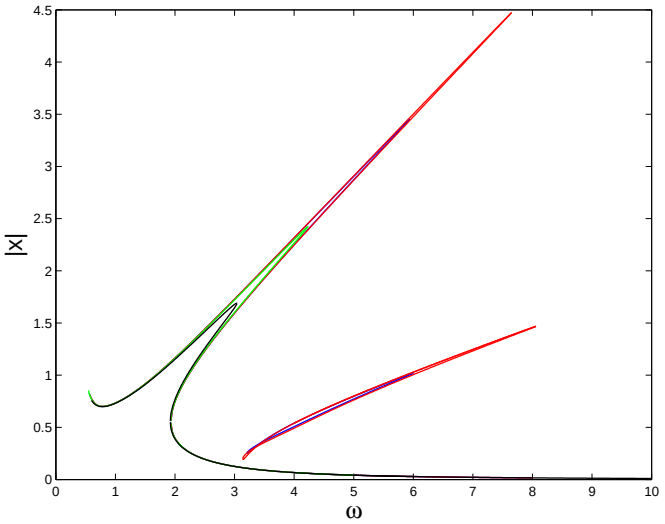

(a) harmonic and $1/3$ subharmonic response for various ξ.

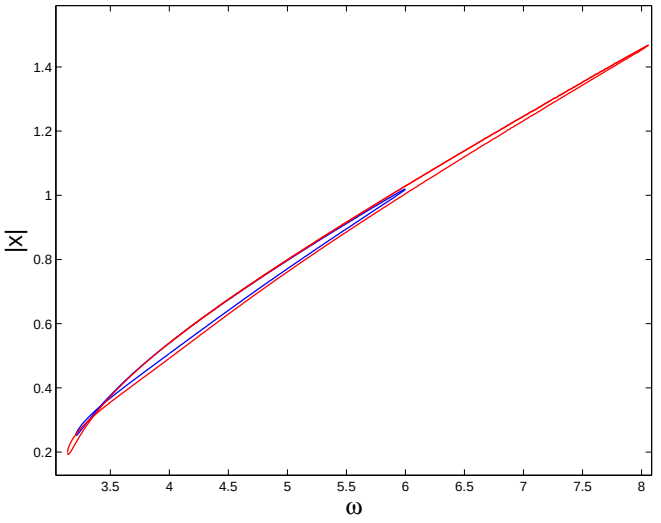

(b) $1/3$ subharmonic response.

Figure 5: The amplitude versus frequency curves of the harmonic and $1/3$ subharmonic solutions for the Duffing equation $\ddot{x}+\xi\dot{x}+x+4x^3=\cos\omega t$, where red curve: $\xi=0.03$; blue curve: $\xi=0.05$; green curve: $\xi=0.1$; black curve: $\xi=0.2$. Note that when $\xi=0.1$ and 0.2, $1/3$ subharmonic response does not occur.

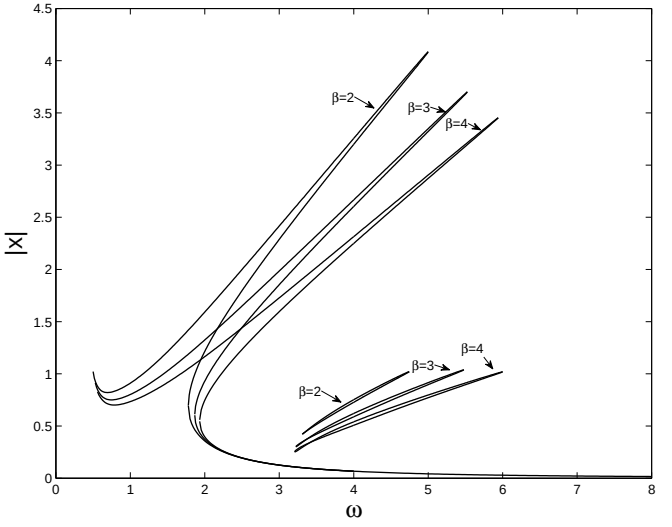

(a) harmonic and $1/3$ subharmonic response for $\beta = 2, 3$ and 4.

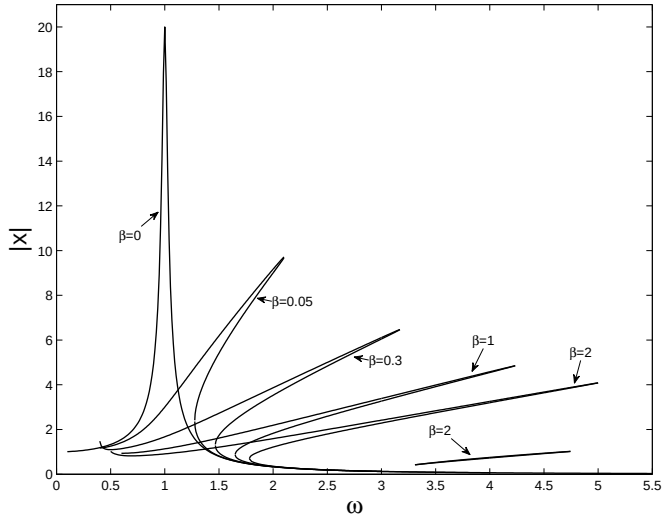

(b) harmonic and $1/3$ subharmonic response for $\beta = 0, 0.05, 0.3, 1$ and 2.

Figure 6: The amplitude versus frequency curves of the harmonic and $1/3$ subharmonic solutions for the Duffing equation $\ddot{x} + 0.05\dot{x} + x + \beta x^3 = \cos \omega t$. Note that the $1/3$ subharmonic response does not exist for $\beta = 0, 0.05, 0.3$ and 1.

infinity as stated in the undamped case. It also indicates that the damping does not bend the curve, which means the response curves for different damping have the same backbone. Fig. 5(a) also reveals that the damping almost does not influence the response curve except elongating the tip area.

Fig. 5(b) is the zoom-in of the subharmonic part in Fig. 5(a). It shows that a larger ξ narrows the occurrence domain of the subharmonic solution. It should be noted that for $\xi = 0.1,\ 0.2$ in this case, the subharmonic solution does not exist. Hence, there exists a certain damping value, greater than which the subharmonic solution disappears.

7.2 The effect of nonlinearity β

Fig. 6 shows the amplitude versus frequency curves of the harmonic and $1/3$ subharmonic solutions for different values of nonlinearity. It shows in Figs. 6(a) and 6(b) that a positive nonlinearity has the effect of bending the response curve to the right. The larger the nonlinearity is, the more the curve bends. It applies to both harmonic and subharmonic response curves.

We also see that the upper branch of the harmonic response, and the subharmonic response are bounded values, which is different from the undamped system. Also, the subharmonic response only exists in a finite frequency domain, which can be influenced by β. Fig. 6(a) indicates that smaller β narrows this domain. Fig. 6(b) shows that when β decreases to a certain value, the subharmonic response ceases to occur.

7.3 The effect of the amplitude F of the impressed force

The effect of the amplitude of the impressed force is shown in Fig. 7. It indicates qualitatively that F does not bend the response curve, which is similar to the damping ξ. Hence, all response curves have the same backbone. What is different from the effect of ξ is that F affects the response globally, while ξ only influences the tip area. As F increases, the peak amplitude of the harmonic response will increase, see Fig. 7(a). Fig. 7(b) shows that a larger F may enlarge the occurrence domain of the subharmonic solution. When F decreases to a certain value, the subharmonic solution ceases to occur. In the current case, when $F = 0.3,\ F = 0.5$ and $F = 1$ the subharmonic solution does not occur. When $F = 1.5$ and $F = 1.8$ it appears. It means a certain value between $1 \sim 1.5$ is the onset of the subharmonic solution.

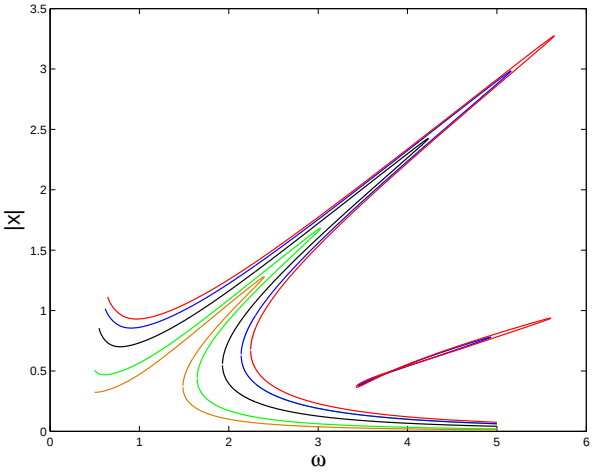

(a) harmonic and $1/3$ subharmonic response for various F.

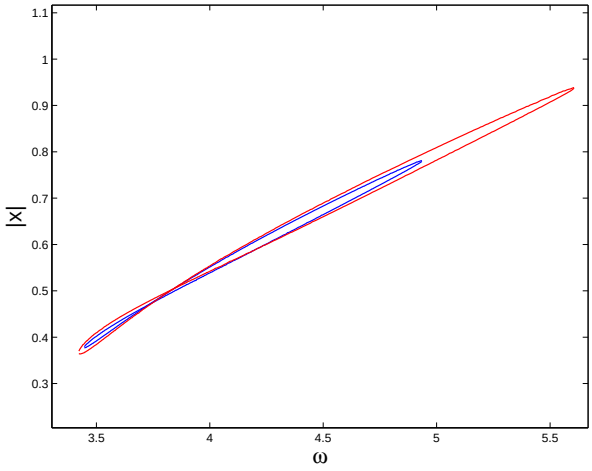

(b) $1/3$ subharmonic response.

Figure 7: The amplitude versus frequency curves of the harmonic and $1/3$ subharmonic solutions for the Duffing equation $\ddot{x}+0.1\dot{x}+x+4x^3 = F\cos\omega t$; the curves (left part of (a)) from bottom to top are $F = 0.3$, $F = 0.5$, $F = 1$, $F = 1.5$ and $F = 1.8$ sequentially. Note that subharmonic response does not occur for $F = 0.3$, $F = 0.5$ and $F = 1$.

8 The comparison of the collocation method and the time Galerkin [Harmonic-Balance] method

In this section, both the collocation method and the time Galerkin [Harmonic-Balance] method are applied to compute the $1/3$ subharmonic solution of Duffing equation. The N-th order approximation is sought as Eq. (13). The residual-error function $R(t)$ is the same as Eq. (14).

In using the Galerkin method, instead of collocating $R(t)$ at $2N$ selected points, we apply the Galerkin procedure over the time domain, i.e., a period of the periodic oscillation, namely $[0,\ 6\pi/\omega]$:

$$\begin{cases} F_j^c(a_1,a_2,\ldots,a_N;b_1,b_2,\ldots,b_N) := \displaystyle\int_0^{6\pi/\omega} R(t)\cos\frac{1}{3}(2j-1)\omega t dt = 0_j, & \text{(57a)} \\ F_j^s(a_1,a_2,\ldots,a_N;b_1,b_2,\ldots,b_N) := \displaystyle\int_0^{6\pi/\omega} R(t)\sin\frac{1}{3}(2j-1)\omega t dt = 0_j, & \text{(57b)} \end{cases}$$

where, $j = 1,2,\ldots,N$. Therefore, we obtain a system of $2N$ nonlinear algebraic equations, i.e. $\begin{bmatrix} \mathbf{F^c} \\ \mathbf{F^s} \end{bmatrix}_{2N\times 1} = \mathbf{0}$. Consequently, the Jacobian matrix $\mathbf{B}$ is

$$\mathbf{B} = \begin{bmatrix} \frac{\partial F_j^c}{\partial a_i} & \frac{\partial F_j^c}{\partial b_i} \\ \frac{\partial F_j^s}{\partial a_i} & \frac{\partial F_j^s}{\partial b_i} \end{bmatrix}_{2N\times 2N} \tag{58}$$

For collocation method, the system of NAEs and its $\mathbf{B}$ are derived very simply. However, the expressions of $\mathbf{F^s}$, $\mathbf{F^c}$ and $\mathbf{B}$ in the time Galerkin [Harmonic-Balance] method are not so easy. Although one can use the harmonic balance principle to simplify the integration procedure, unfortunately the cubic term in the Duffing equation has to be expanded into Fourier expansions, which calls for heavy symbolic operations. The larger N is, the heavier the symbolic operations will be. Derivations of $\mathbf{F^s}$, $\mathbf{F^c}$ and $\mathbf{B}$ are provided in the Appendix.

For comparison, we solve $\ddot{x}+0.05\dot{x}+x+4x^3 = \cos 4t$, by the fourth order Runge-Kutta method (RK4), the collocation method, and the Galerkin Harmonic-Balance method. Fig. 8(a) plots the phase portraits of the Duffing equation by the three methods. Fig. 8(b) provides the x versus t curves. We can see from Fig. 8 that both the collocation method and the Galerkin method agree very well with the RK4, which serves as the benchmark here.

For the comparison in Fig. 8(b), the numerical integration, i.e. RK4, is firstly performed over a sufficient long time, e.g. 1000s, to damp out the transient motion. Next, we need to adjust the starting point of the solution of RK4 so as to compare with the other two methods. We calculate the starting values $x(0) =$

Table 4: Comparison of peak amplitudes by Galerkin method and RK4

ORDER	GALERKIN	RK4	ERROR[3]
$N=5$	0.506867205983612	0.506867056360695	2.95192×10^{-7}
$N=10$	0.506867055901930	0.506867056360695	9.05099×10^{-10}
$N=15$	0.506867055901947	0.506867056360695	9.05687×10^{-10}

Table 5: Comparison of peak amplitudes by collocation method and RK4

ORDER	COLLOCATION	RK4	ERROR
$N=5$	0.506936844520838	0.506867056360695	1.37685×10^{-4}
$N=10$	0.506870868174788	0.506867056360695	7.52034×10^{-6}
$N=15$	0.506867255577109	0.506867056360695	3.93035×10^{-7}

0.449685433055615, $\dot{x}(0)=0.160947174961521$ of the solution by the collocation method, and $x(0)=0.449685425459622$, $\dot{x}(0)=0.160850450654150$ of the solution by the Galerkin method.

In the computer program, performing the numerical integration starting at $t=1000s$, we record the time t_0 such that $|x(t_0)-0.4496854|<10^{-6}$ and $|x(t_0)-0.1609|<10^{-3}$. In computation, t_0 is 1004.131539914663; the time t_0 is used as the starting point of the RK4 in Fig. 8(b). The numerical integration is then performed over $[t_0,t_0+6\pi/\omega]$ to generate a periodic solution. It should be pointed out that the x vs t curves by collocation method and Galerkin method are shifted by t_0 in Fig. 8(b) for comparison.

To further compare the two methods, Fig. 9 gives the difference of x in absolute value between collocation method and Galerkin method. We can see that maximum differences between the two methods for order $N=5,\ 10$ and 15 are about 7.82×10^{-5}, 3.82×10^{-6} and 2.39×10^{-7} respectively. It should be mentioned that the RK4 is not applied as the benchmark in this level of comparison in Fig. 9, since one can not obtain the exact starting time of RK4 to compare with collocation method and Galerkin method.

However, we can compare the peak amplitudes by collocation method and Galerkin method with that by RK4, because the very accurate amplitude of x by RK4 is easy to get. Tables 4 and 5 tabulate the peak amplitudes by Galerkin method, the collocation method and the RK4. It is demonstrated from Tables 4 and 5 that both the Galerkin method and the collocation method are very accurate by comparing

[3] ERROR=$\frac{|x_{Galerkin}-x_{RK4}|}{|x_{RK4}|}$, where $|x_{Galekrin}|$ denotes the peak amplitude by Galerkin method and $|x_{RK4}|$ denotes the peak amplitude by RK4. Similar definition is made in Table 5.

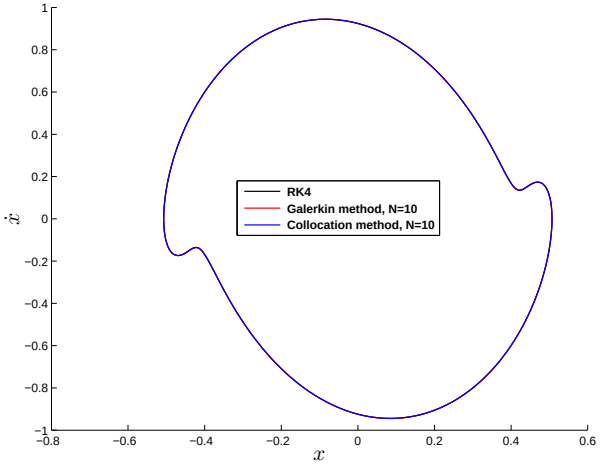

(a) Phase portraits by the RK4, the Galerkin method and the collocation method.

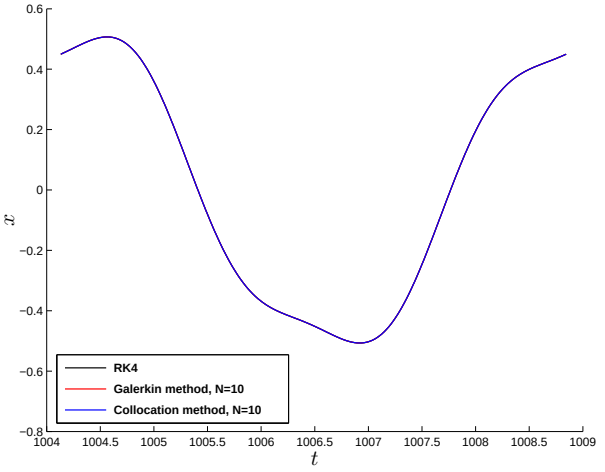

(b) x vs t

Figure 8: The $1/3$ subharmonic solutions by the fourth order Runge-Kutta method, the Galerkin method and the collocation method for Duffing equation $\ddot{x}+0.05\dot{x}+x+4x^3=\cos 4t$: (a) phase portraits; (b) x evolves with time t. Figures show that the three methods coincide with each other.

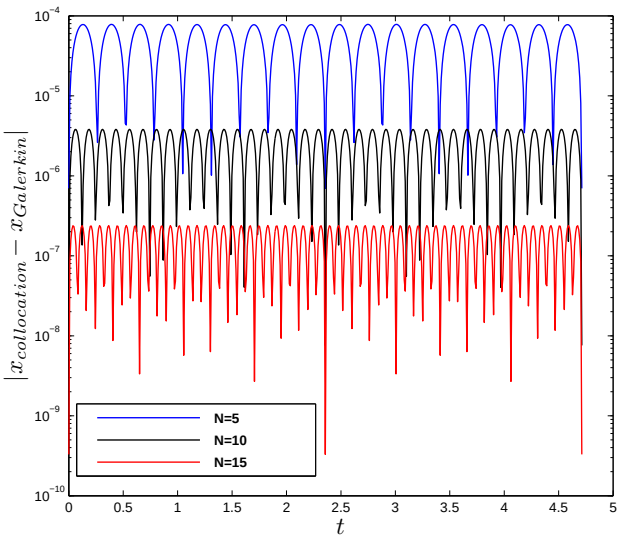

Figure 9: The difference of x in absolute value between the collocation method and the Galerkin method.

with RK4. Concretely, we can see from Table 5 that the collocation method with $N = 10$ and $N = 15$ can yield highly accurate solutions with errors of the order about 10^{-6} and 10^{-7}, respectively.

9 Conclusions

In this paper, we proposed a simple collocation method. The collocation method was applied to find the harmonic and $1/3$ subharmonic periodic solutions of the Duffing equation. The collocation of the residual error in the ODE, at discrete time intervals, was performed on a whole period of the considered oscillation. After collocation, the resulting nonlinear algebraic equations were solved by the Newton-Raphson method. To start with, the initial values for the higher order approximation were provided by solving the second order approximation, which lead to the corresponding higher order solutions. The non-physical solution phenomenon disappeared. Based on the proposed scheme, we effectively found the frequency response, and then thoroughly investigated the effect of each parameter in the Duffing equation. Besides, the relation between the collocation method and the HDHB was explored. We first demonstrated that the HDHB is actually a transformed collocation method. The numerical integration method was applied to compare with the collocation method, and the time Galerkin [Harmonic-Balance] method. It verified the high accuracy of both methods. However, the collocation

method is much simpler than the Galerkin [Harmonic-Balance] method. Numerical examples confirmed the simplicity and effectiveness of the present scheme. In summary, this method is superior to the HDHB and the HB. It can be readily applied to seek any order of subharmonic, superharmonic and ultrasubharmonic solutions.

Acknowledgement: The first author gratefully acknowledges the guidance from Professor Atluri, and the support from the Northwestern Polytechnical University. At UCI, this research was supported by the Army Research Laboratory, with Drs. A. Ghoshal and Dy Le as the Program Officials. This research was also supported by the World Class University (WCU) program through the National Research Foundation of Korea funded by the Ministry of Education, Science and Technology (Grant no.: R33-10049). The work of the second author at UCI was funded by the US Air Force.

References

Atluri, S. N. (2004): *The meshless method (MLPG) for domain & BIE discretizations*, volume 677. Tech Science Press.

Atluri, S. N. (2005): *Methods of computer modeling in engineering & the sciences*. Tech Science Press.

Atluri, S. N.; Shen, S. (2002): *The meshless local Petrov-Galerkin (MLPG) method*. Crest.

Atluri, S. N.; Zhu, T. (1998): A new meshless local Petrov-Galerkin (MLPG) approach in computational mechanics. *Comput. Mech.*, vol. 22, pp. 117–127.

Dai, H. H.; Paik, J. K.; Atluri, S. N. (2011a): The global nonlinear galerkin method for the analysis of elastic large deflections of plates under combined loads: A scalar homotopy method for the direct solution of nonlinear algebraic equations. *Computers Materials and Continua*, vol. 23, no. 1, pp. 69.

Dai, H. H.; Paik, J. K.; Atluri, S. N. (2011b): The Global Nonlinear Galerkin Method for the Solution of von Karman Nonlinear Plate Equations: An Optimal & Faster Iterative Method for the Direct Solution of Nonlinear Algebraic Equations $\mathbf{F}(\mathbf{x}) = \mathbf{0}$, using $\mathbf{x} = \lambda\ [\alpha\mathbf{F} + (1-\alpha)\mathbf{B}^T\mathbf{F}]$. *Computers Materials and Continua*, vol. 23, no. 2, pp. 155.

Ekici, K.; Hall, K.C. (2011): Harmonic balance analysis of limit cycle oscillations in turbomachinery. *AIAA journal*, vol. 49, no. 7, pp. 1478–1487.

Ekici, K.; Hall, K.C.; Dowell, E.H. (2008): Computationally fast harmonic balance methods for unsteady aerodynamic predictions of helicopter rotors. *Journal of Computational Physics*, vol. 227, no. 12, pp. 6206–6225.

Hall, K. C.; Thomas, J. P.; Clark, W. S. (2002): Computation of unsteady nonlinear flows in cascades using a harmonic balance technique. *AIAA Journal*, vol. 40, pp. 879–886.

Hayashi, C. (1953a): Forced oscillations with nonlinear restoring force. *Journal of Applied Physics*, vol. 24, no. 2, pp. 198–207.

Hayashi, C. (1953b): Stability investigation of the nonlinear periodic oscillations. *Journal of Applied Physics*, vol. 24, no. 3, pp. 344–348.

Hayashi, C. (1953c): Subharmonic oscillations in nonlinear systems. *Journal of Applied Physics*, vol. 24, no. 5, pp. 521–529.

Levenson, M. E. (1949): Harmonic and subharmonic response for the Duffing equation: $\ddot{x}+\alpha x+\beta x^3 = F\cos\omega t(\alpha > 0)$. *Journal of Applied Physics*, vol. 20, no. 11, pp. 1045–1051.

Liu, C. S.; Dai, H. H.; Atluri, S. N. (2011a): Iterative Solution of a System of Nonliear Albegraic Equations $\mathbf{F}(\mathbf{x}) = \mathbf{0}$, using $\dot{\mathbf{x}} = \lambda[\alpha\mathbf{R}+\beta\mathbf{P}]$ or $\lambda[\alpha\mathbf{F}+\beta\mathbf{P}^*]$, $\mathbf{R}$ is normal to a Hyper-Surface Function of $\mathbf{F}$, $\mathbf{P}$ Normal to $\mathbf{R}$, and $\mathbf{P}^*$ Normal to $\mathbf{F}$. *CMES: Computer Modeling in Engineering & Sciences*, vol. 81, no. 4, pp. 335–362.

Liu, C. S.; Dai, H. H.; Atluri, S. N. (2011b): A further study on using $\dot{\mathbf{x}} = \lambda[\alpha\mathbf{R}+\beta\mathbf{P}]$ ($\mathbf{P} = \mathbf{F} - \mathbf{R}(\mathbf{F}\cdot\mathbf{R})/\|\mathbf{R}\|^2$) and $\dot{\mathbf{x}} = \lambda[\alpha\mathbf{F}+\beta\mathbf{P}^*]$ ($\mathbf{P}^* = \mathbf{R} - \mathbf{F}(\mathbf{F}\cdot\mathbf{R})/\|\mathbf{F}\|^2$) in iteratively solving the nonlinear system of algebraic equations $\mathbf{F}(\mathbf{x}) = \mathbf{0}$. *CMES: Computer Modeling in Engineering & Sciences*, vol. 81, no. 2, pp. 195–227.

Liu, L.; Dowell, E.H.; Hall, K. (2007): A novel harmonic balance analysis for the van der pol oscillator. *International Journal of Non-Linear Mechanics*, vol. 42, no. 1, pp. 2–12.

Liu, L.; Dowell, E. H.; Thomas, J. P.; Attar, P.; Hall, K. C. (2006): A comparison of classical and high dimensional harmonic balance approaches for a Duffing oscillator. *Journal of Computational Physics*, vol. 215, pp. 298–320.

Liu, L.; Kalmár-Nagy, T. (2010): High-dimensional harmonic balance analysis for second-order delay-differential equations. *Journal of Vibration and Control*, vol. 16, no. 7-8, pp. 1189–1208.

Ludeke, C. A.; Cornett, J. E. (1966): A computer investigation of a subharmonic bifurcation point in the Duffing equation. *J. Appl. Math.*, vol. 14, no. 6, pp. 1298–1306.

Moriguchi, H.; Nakamura, T. (1983): Forced oscillations of system with nonlinear restoring force. *Journal of the Physical Society of Japan*, vol. 52, no. 3, pp. 732–743.

Stoker, J. J. (1950): *Nonlinear Vibrations*. Interscience.

Sturrock, P. A. (1957): Non-linear effects in electron plasmas. *Proceedings of the Royal Society of London. Series A. Mathematical and Physical Sciences*, vol. 242, no. 1230, pp. 277–299.

Thomas, J.P.; Dowell, E.H.; Hall, K.C. (2004): Modeling viscous transonic limit-cycle oscillation behavior using a harmonic balance approach. *Journal of aircraft*, vol. 41, no. 6, pp. 1266–1274.

Thomas, J.P.; Hall, K.C.; Dowell, E.H. (2003): A harmonic balance approach for modeling nonlinear aeroelastic behavior of wings in transonic viscous flow. *AIAA paper*, vol. 1924, pp. 2003.

Thomas, J. P.; Dowell, E. H.; Hall, K. C. (2002): Nonlinear inviscid aerodynamic effects on transonic divergence, futter, and limit-cycle oscillations. *AIAA Journal*, vol. 40, pp. 638–646.

Tseng, W. Y.; Dugundji, J. (1970): Nonlinear vibrations of a beam under harmonic excitation. *Journal of applied mechanics*, vol. 37, no. 2, pp. 292–297.

Tseng, W. Y.; Dugundji, J. (1971): Nonlinear vibrations of a buckled beam under harmonic excitation. *Journal of applied mechanics*, vol. 38, no. 2, pp. 467–476.

Urabe, M. (1965): Galerkin's procedure for nonlinear periodic systems. *Arch. Rational Mech. Anal.*, vol. 20, pp. 120–152.

Urabe, M. (1969): Numerical investigation of subharmonic solutions to Duffing's equation. *Publ. RIMS Kyoto Univ*, vol. 5, pp. 79–112.

Urabe, M.; Reiter, A. (1966): Numerical computation of nonlinear forced oscillations by Galerkin's procedure. *J. Math. Anal. Appl*, vol. 14, pp. 107–140.

Appendix A:

$$\begin{cases} a_1\left[36-4\omega^2+27\beta\left(a_1^2+a_1a_2+2a_2^2+b_1^2+2b_1b_2+2b_2^2\right)\right] \\ =-3b_1\left(4\xi\omega-9\beta a_2b_1\right) \\ \\ b_1\left[36-4\omega^2+27\beta\left(a_1^2+2a_2^2-2a_1a_2+b_1^2-b_1b_2+2b_2^2\right)\right] \\ =3a_1\left(4\xi\omega-9\beta a_1b_2\right) \\ \\ a_2\left[4-4\omega^2+3\beta\left(2a_1^2+a_2^2+2b_1^2+b_2^2\right)\right]=4F-4b_2\omega\xi-\beta a_1\left(a_1^2-3b_1^2\right) \\ \\ b_2\left[4-4\omega^2+3\beta\left(2a_1^2+a_2^2+2b_1^2+b_2^2\right)\right]=\beta b_1\left(b_1^2-3a_1^2\right)+4\omega\xi a_2. \end{cases} \tag{59}$$

Appendix B:

$$\begin{cases} A_1\left[4-4\omega^2+3\beta\left(A_1^2+A_1A_2+2A_2^2+B_1^2+2B_1B_2+2B_2^2\right)\right] \\ =4F+B_1\left(3\beta A_2B_1-4\xi\omega\right) \\ \\ B_1\left[4-4\omega^2+3\beta\left(A_1^2-2A_1A_2+2A_2^2+B_1^2-B_1B_2+2B_2^2\right)\right] \\ =4\,\xi\omega A_1-3\beta A_1^2B_2\big) \\ \\ A_2\left[4-36\omega^2+3\beta\left(2A_1^2+A_2^2+2B_1^2+B_2^2\right)\right]=\beta A_1\left(3B_1^2-A_1^2\right)-12\xi\omega B_2 \\ \\ B_2\left[4-36\omega^2+3\beta\left(2A_1^2+A_2^2+2B_1^2+B_2^2\right)\right]=12\xi\omega A_2+\beta B_1\left(B_1^2-3A_1^2\right). \end{cases} \tag{60}$$